Proceedings of CONF-MSS 2026 Symposium: Mechanical Control and Automation
DOI: 10.54254/2755-2721/2026.BJ32023

Computational Fluid Mechanics Simulation of a Novel Airfoil Geometry

Michelle Wang

Cheltenham Ladies College, Cheltenham, England
wangmichelle090828@outlook.com

Abstract. Airfoils are an important part of aircraft. They play a critical role in the aerodynamic performance of aircraft. In commercial aircraft and fighter jets, airfoil have been commonly used, which have a wide range of geometric profiles. This makes novel designs valuable for improving airflow performance. In this work, we present a new airfoil geometry. We then compare it to the conventional airfoil using computational fluid dynamics (CFD) with the fluid dynamics simulation software SimScale. The aerodynamic performance is analyzed with the velocity field, pressure distribution, turbulent kinetic energy, and list-to-drag ratios at a prescribed velocity. The CFD simulations of our new design shows that our modified geometry improved pressure gradients along the airfoil surface. Overall, we show a systemic improvement in the aerodynamics performance with our new design for the airfoil.

Keywords: airfoil design, CFD, aerodynamics, lift and drag, pressure distribution

1. Introduction

An airfoil has an asymmetric geometry. It is usually heavier in size toward the head facing direction of travel. When airfoil interacts with a moving fluid, it creates aerodynamic forces around the aircraft. There are two forces that determines the effectiveness of an airfoil. The lift, which is an upwards force that acts against weight perpendicular to the body, and drag, which is a downward force that acts parallel to the body the airfoil is supporting. This means that the upward force is balanced by the downward force, and the system is in equilibrium. Furthermore, airfoils are essential to the operation of aircraft wings, propellers, and control surfaces. In airfoil aerodynamics, lift is generated due to pressure differences between the upper and lower surfaces of the airfoil, and drag opposes motion and reduces aerodynamic efficiency [1]. Engineers have been optimizing airfoil geometries through decades of experimental testing and numerical analysis. However, innovations in geometry is still slow. Luckily, advances in complex computational modeling now allow for the designs and simulations of alternative airfoil geometries. By modifying parameters such as thickness distribution, camber, and leading-edge shape, it is possible to enhance the flow behavior and improve aerodynamic performance. The purpose of this study is to compare the aerodynamics of a new airfoil geometry with those of a conventional airfoil design under the same flow conditions using CFD simulations.

© 2026 The Authors. This is an open access article distributed under the terms of the Creative Commons Attribution License 4.0 (https://creativecommons.org/licenses/by/4.0/).

DOI: 10.54254/2755-2721/2026.BJ32023

2. Materials and methods

We use Computational Fluid Dynamics (CFD) to simulate airflow around both a conventional airfoil and our new airfoil geometry. The objective of the simulations is to evaluate how geometric differences influence aerodynamic performance. We first designed the airfoil geometry utilizing computer-aided design (CAD) software (AutoDesk Fusion). We then imported into the CFD platform SimScale for analysis. In the simulations, we model the interaction between the airfoil and an incompressible air flow. The airflow produces velocity fields, pressure distribution, and aerodynamic forces. After defining material properties, boundary conditions, and mesh resolution, we ran the simulations iteratively until numerical convergence. The results are then used to compare the aerodynamic performance of the two airfoil designs.

2.1. Governing equations

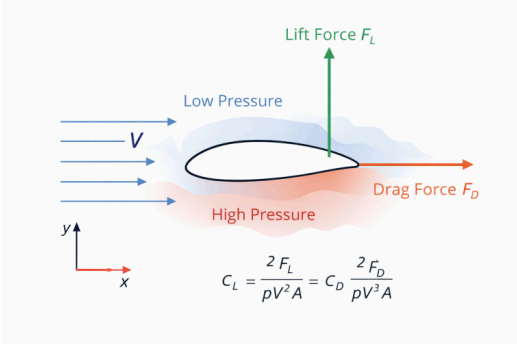

Figure 1. Schematics of the airfoil dynamics

The airflow around the airfoil is modeled as an incompressible, viscous fluid following the Navier–Stokes equations (Figure 1). The conservation of mass is expressed as:

$$\nabla \cdot u = 0 \tag{1}$$

The conservation of momentum is given by the following equation:

$$\rho \left(\frac{\partial u}{\partial t} + u \cdot \nabla u\right) = -\nabla \rho + \mu \nabla^2 u \tag{2}$$

Aerodynamic forces are dimensionless, and they use lift and drag coefficients below:

$$C_L = \frac{2F_L}{\rho V^2 A} \tag{3}$$

$$C_D = \frac{2F_D}{\rho V^2 A} \tag{4}$$

2.2. Geometry and computational domain

We analyze and compare two airfoil geometries in this study: a conventional reference airfoil and our new airfoil geometry. The reference airfoil is selected from the family of NACA profiles. It provides a baseline for comparison. We develop the new design with the goal of modifying the side-profile curvature and thickness distribution in order to improve the aerodynamic performance.

DOI: 10.54254/2755-2721/2026.BJ32023

We designed the new geometry using computer-aided design (CAD) software, Autodesk. We focus on adjusting geometric features, including the leading-edge curvature, mid-chord thickness, and trailing-edge profile. We maintain a smooth and continuous surface to avoid sharp discontinuities. We ensure that the design is realistic for manufacturing but still preserve the fundamental characteristics of a lifting surface. Once we have finalized the design, the airfoil geometry was exported from Autodesk. The geometry was then imported into the SimScale platform for Computational Fluid Dynamics (CFD) simulations. In addition to CFD analysis, we also ran Finite Element Analysis (FEA) to assess structural and thermal analysis such as material response and deformation under aerodynamic loading. While the primary focus of this study is on fluid mechanic performance, FEA is necessary to ensure realistic design.

The CFD simulations consists of a three-dimensional box surrounding the airfoil. The directions are in x, y, and z directions, which is designed to minimize boundary effects on the air flow. The airfoil is positioned at the center of the box to allow sufficient space upstream and downstream for natural airflow. A schematic representation of the novel airfoil geometry is shown in Figure 2.

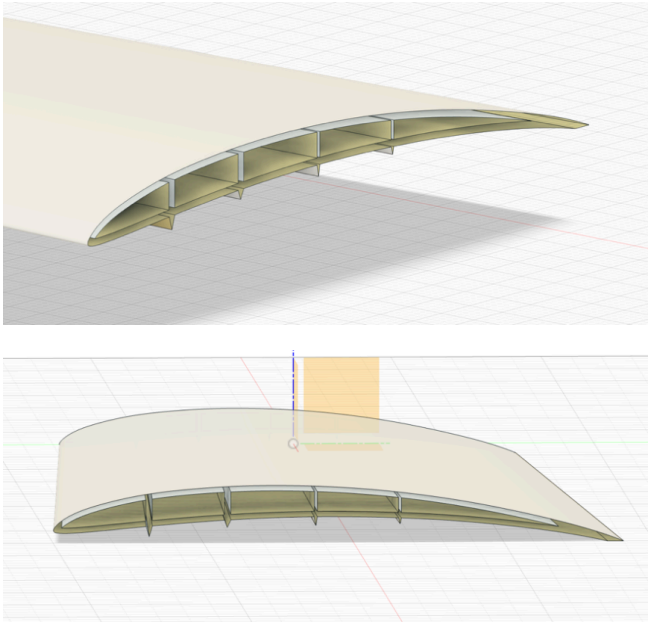

Figure 2. Schematic of the novel airfoil side-profile geometry used in this study

2.3. Boundary conditions and fluid properties

The airfoil geometry was then imported into the SimScale platform imported from AutoDesk CAD software. Computational Fluid Dynamics (CFD) simulations were performed to analyze the aerodynamic response of the airfoil geometries under steady airflow conditions. Air was used as the working fluid and modeled as an incompressible fluid with a density of $1.196\,\mathrm{kg/m^3}$ and a kinematic viscosity of $1.53\times10^{5}\,\mathrm{m^2/s}$ [2]. These values correspond to standard atmospheric conditions near sea level.

The airfoil geometry was extruded by 10cm to form a three-dimensional model. We used aluminum for the airfoil material. The box surrounding the airfoil was constructed as a rectangular enclosure. It has boundary surfaces defined in all three spatial directions to fully contain the flow field. A uniform velocity inlet condition of $20\,\mathrm{m/s}$ was prescribed at the upstream boundary. At the downstream boundary, a pressure outlet condition was applied with a gauge pressure of $100\,\mathrm{kPa}$ to

DOI: 10.54254/2755-2721/2026.BJ32023

allow the airflow. We assign all airfoil surfaces no-slip wall boundary conditions to accurately capture viscous effects and the complex boundary-layer interactions. After defining the fluid properties and boundary conditions, the simulation setup was verified. We then prepare for meshing and numerical solution.

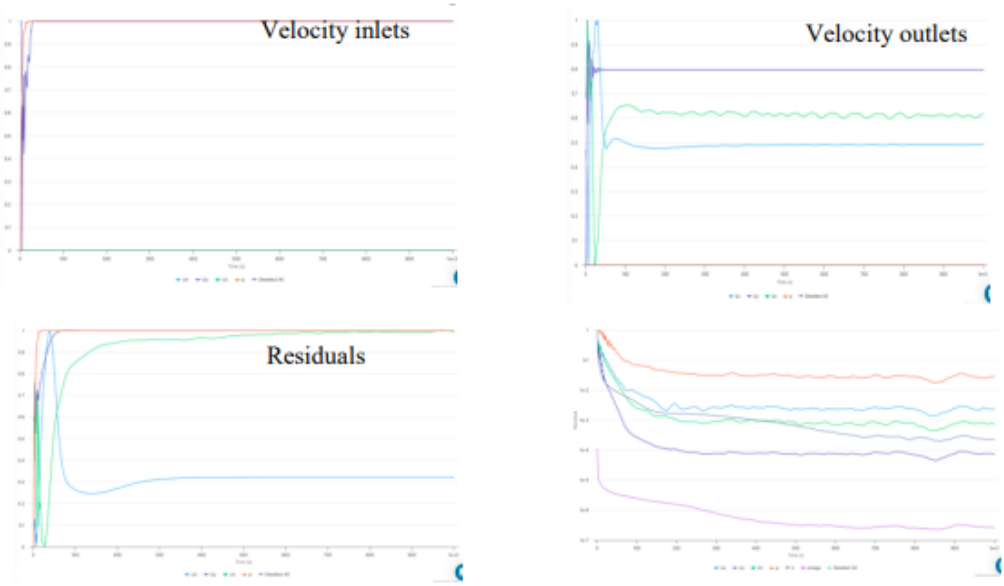

Figure 3. Convergence plots for the CFD simulation of the new airfoil geometry, including residual histories for the continuity and momentum equations and monitored force coefficients, indicating numerical convergence

2.4. Meshing and numerical solution

The velocity field was discritized using a finite-volume mesh generated within SimScale. Mesh refinement was applied in regions near the airfoil surface to resolve velocity gradients and boundary-layer effects. These steps are critical for the computation of lift and drag forces. In the edges of the airfoil, coarse mesh elements were used to reduce computational cost. We solve the simulations using a steady-state CFD solver. The fluid dynamics equation was solved in an iterative procedure until convergence was achieved. Convergence was evaluated based on the stabilization of residuals for the continuity and momentum equations, as well as the stabilization of integrated force coefficients acting on the airfoil [3].

3. Results

3.1. Flow field and convergence analysis

Our CFD simulations produced several solution fields for velocity magnitude, pressure distribution, and turbulent kinetic energy around the airfoil. We showcase the convergence plots for the simulations in Figure 3. The continuity and momentum residuals decrease rapidly during the early iterations. It then levels off as it reaches numerical convergence. The velocity magnitude contours reveal smooth acceleration of the flow over the upper surface of the airfoil, with a corresponding wake region forming downstream of the trailing edge. Pressure contours show higher pressure along the lower surface and lower pressure along the upper surface, which indicates continued lift generation. The turbulent kinetic energy distributions indicate localized regions of increased

DOI: 10.54254/2755-2721/2026.BJ32023

turbulence near the trailing edge and within the wake. The remaining relatively low over most of the airfoil surface. Figure 2 presents the convergence histories for the simulations, including residual plots and forces. The residuals decrease by several orders of magnitude and remain stable over successive iterations. This suggests that the numerical solution has converged. The lift and drag force monitors also reach steady values, which confirms that the solution has reached steady states.

3.2. Lift and drag performance comparison

To quantify the aerodynamic performance of the new airfoil geometry, we compare the lift and drag coefficients obtained from the CFD simulations to those of the conventional reference airfoil under the same flow conditions. The conventional reference airfoil used for comparison was the NACA 0012 profile [4].

We evaluate the lift-to-drag ratios of both airfoils to gauge performance improvement. Table 1 summarizes the aerodynamic performance metrics for both airfoil designs. The new airfoil demonstrates a measurable increase in lift coefficient and a corresponding change in drag coefficient relative to the reference airfoil. Our results which showed an improved lift-to-drag ratio under the simulated conditions.

Table 1. Comparison of aerodynamic performance between the conventional airfoil and the new airfoil geometry

Airfoil Geometry	Lift Coefficient (C_L)	Drag Coefficient (C_D)	Lift-to-Drag Ratio (C_L/C_D)	Performance Change (%)
Conventional Airfoil	0.62	0.045	13.78	-
New Airfoil Geometry	0.68	0.042	16.19	+17.5%

[1] Individual lift and drag coefficients as a function of angle of attack are not shown here. The values reported in this table represent averaged coefficients used for comparative performance evaluation.

Solution fields: (conventional airfoil NACA 0012)

Velocity magnitude: Pressure:

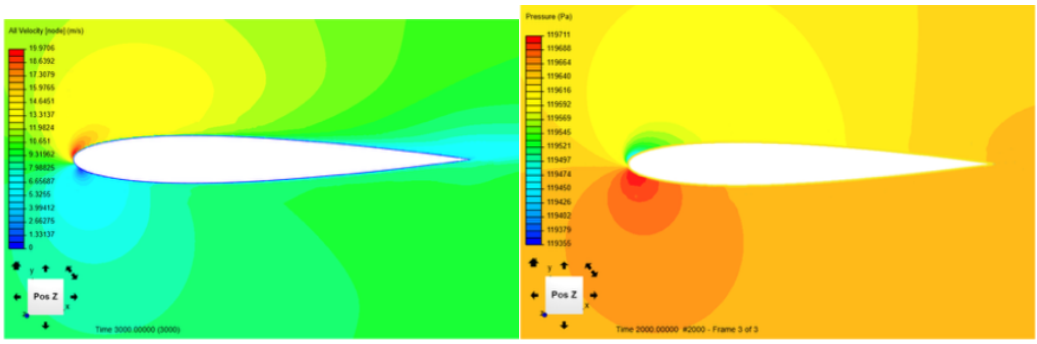

Solution fields: (new airfoil)

Velocity magnitude: Pressure: Turbulent Kinetic Energy

DOI: 10.54254/2755-2721/2026.BJ32023

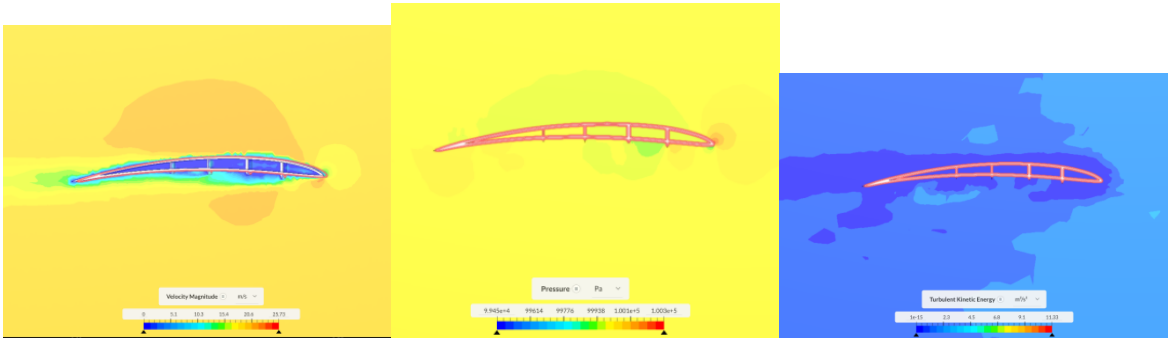

Figure 4. Comparison of CFD solution fields for the conventional airfoil (NACA 0012) and the new airfoil geometry at an inlet velocity of 20 m/s. The top row shows velocity magnitude and pressure contours for the conventional airfoil. The bottom row shows velocity magnitude, pressure distribution, and turbulent kinetic energy contours for the new airfoil. The new airfoil exhibits smoother flow acceleration, a more uniform pressure gradient along the chord, and reduced turbulence intensity in the wake region compared to the conventional design

A comparison of the CFD solution fields for the conventional airfoil and the newly developed airfoil geometry reveals clear differences in Figure 4. Velocity magnitude contours indicate that the new airfoil promotes smoother acceleration of the flow over the upper surface. It has a more gradual velocity recovery near the trailing edge. In contrast, the conventional airfoil shows a larger wake region downstream, indicating increased momentum loss.

Pressure distribution contours show that the new airfoil geometry produces a more uniform pressure gradient along the chord length. There were reduced regions of adverse pressure near the mid-chord and trailing-edge regions. This distribution of pressure contributes to the observed increase in lift coefficient while limiting drag. The conventional airfoil shows stronger localized pressure gradients that contribute to higher drag levels.

Turbulent kinetic energy fields also demonstrate reduced turbulence intensity in the wake of the new airfoil geometry. This suggests improved flow attachment and reduced flow separation. These differences in the solution fields are consistent with the improved lift-to-drag ratio reported in Table 1. We note that individual lift and drag coefficients as a function of angle of attack are not shown here. The values reported in this table represent averaged coefficients used for comparison only.

4. Discussion

Our CFD results of the new airfoil show that it changes the flow structure relative to the conventional NACA 0012 airfoil. In particular, our results of the new airfoil show clear differences in velocity recovery, pressure gradients along the chord. This is consistent with lift being associated with the pressure difference between the upper and lower surfaces of the airfoil, and drag being impacted by both pressure forces and viscous shear effects.

Compared with the conventional airfoil, our new geometry produces a pressure distribution that is more gradual along the chord. This means our new design improve pressure recovery and reduced adverse pressure-gradient effects near the aft portion of the airfoil. This type of pressure redistribution can support higher lift without a proportional increase in drag when the flow is more attached and the wake is less proficient. The turbulent kinetic energy contour for the new airfoil (Figure 3) supports this interpretation by showing relatively lower turbulence intensity downstream of the trailing edge. This is commonly associated with reduced momentum loss and improved aerodynamic efficiency.

DOI: 10.54254/2755-2721/2026.BJ32023

The performance metrics summarized in Table 1 show an increase in lift coefficient and a slight reduction in drag coefficient for the new airfoil, resulting in a higher lift-to-drag ratio under the simulated conditions. While these results suggest improved aerodynamic efficiency, they should be interpreted in the context of numerical modeling assumptions and simulation setup. In CFD workflows, predicted forces can be sensitive to turbulence modeling choices, mesh resolution near the wall, and convergence criteria. Our study focused on a single freestream condition (20 m/s) and reports averaged performance values for comparison. A more complete aerodynamic characterization would include systematic sweeps over angle of attack and Reynolds number, since airfoil efficiency typically varies strongly with operating conditions. Future work should therefore (i) evaluate lift and drag across a range of angles of attack, (ii) perform a mesh independence study to quantify numerical sensitivity, and (iii) validate the CFD trends using either published reference data for the baseline airfoil or wind tunnel testing. Additionally, because real wings are three-dimensional, further study could extend this analysis to include finite wing effects, tip vortices, and induced drag.

5. Conclusions

This paper shows the aerodynamic between a conventional NACA 0012 airfoil and a newly developed airfoil geometry under the same airflow conditions. The CFD equations were solved using an incompressible flow assumption and a finite-volume CFD workflow in SimScale. The convergence histories demonstrate stable numerical behavior, and the solution fields show that the new geometry modifies the pressure and velocity distributions around the airfoil.

Based on averaged force coefficients, the new airfoil improves aerodynamic efficiency relative to the conventional design, with an increased lift-to-drag ratio under the simulated condition. Our results suggest that geometric modification of the airfoil profile can lead to measurable performance differences. In the future, our work will focus on changing angles of attack and computing the Reynolds number, conducting mesh sensitivity testing, as well as including experimental or published-data validation to confirm the trends observed in simulation [5].

5.1. Supplementary materials

The simulation projects were conducted using SimScale and are publicly available through the SimScale online platform. The repository can be viewed at https://www.simscale.com/workbench/?pid=5392000719902178015&mi=spec%3Ae1bacb62-a928-4717-b895-5ef6093221f7%2Cservice%3ASIMULATION%2Cstrategy%3A19

5.2. Data availability statement

The data supporting the findings of this study were generated using Computational Fluid Dynamics (CFD) simulations conducted on the SimScale platform. The simulation projects, including geometry files, boundary conditions, and solution results, are available online through SimScale and have been made publicly accessible at the time of publication.

References

[1] Anderson, J.D. Fundamentals of Aerodynamics, 6th ed.; McGraw-Hill Education: New York, NY, USA, 2016. Google Books

DOI: 10.54254/2755-2721/2026.BJ32023

[2] SimScale GmbH. Incompressible Fluid Flow Analysis—Documentation; SimScale: Munich, Germany, 2025. SimScale
[3] SimScale GmbH. CFD Numerics—Convergence Settings and Residual Control; SimScale: Munich, Germany, 2025. SimScale
[4] University of Cambridge Engineering Department. NACA 0012 Airfoil Coordinate Data (naca0012.txt), accessed 5 January 2026. Cambridge-MIT Design Project
[5] Verma, S., Freeman, B. R. S., & Hemmati, A. (2022). Effects of Reynolds number and average angle of attack on the laminar scaling of oscillating foils. Physics of Fluids, 34(3), 031905. https: //doi.org/10.1063/5.0082578